PRAMANA
— journal of
physics

Vol. 67, No. 1
July 2006
pp. 121–134

Langmuir Blodgett multilayers and related nanostructures

S S MAJOR[1], S S TALWAR[1] and R S SRINIVASA[2]
[1]Department of Physics; [2]Department of Metallurgical Engineering and Materials Science, Indian Institute of Technology Bombay, Mumbai 400 076, India
E-mail: syed@phy.iitb.ac.in

Abstract. Langmuir Blodgett (LB) process is an important route to the development of organized molecular layered structures of a variety of organic molecules with suitably designed architecture and functionality. LB multilayers have also been used as templates and precursors to develop nano-structured thin films. In this article, studies on the molecular packing and three-dimensional structure of prototypic cadmium arachidate (CdA), zinc arachidate (ZnA) and mixed CdA–ZnA LB multilayers are presented. The formation of semiconducting nano-clusters of CdS, ZnS and $Cd_xZn_{1-x}S$ alloys within the organic multilayer matrix, using arachidate LB multilayers as precursors is also discussed.

Keywords. Langmuir Blodgett; multilayers; II–VI semiconductors; nanoclusters.

PACS Nos 68.47.Pe; 81.07.-b; 78.66.Hf

1. Introduction

Organic multilayers deposited by the Langmuir–Blodgett (LB) technique have been the subject of intense research due to the rich variety of organized molecular layered structures they provide [1,2]. Long chain fatty acids and their divalent arachidate/stearate metal salts such as cadmium arachidate (CdA) have been the most extensively studied LB systems and their three-dimensional structure and molecular packing have been investigated using a variety of techniques [3–10]. The molecular packing in the divalent metal fatty acid salt multilayers has been reported [3] to depend on the electronegativity of the metal ion and in most cases, corresponds to the closed packed structures proposed by Kitaigorodskii [11] for long chain organic compounds. These structures are based on orthorhombic, monoclinic and triclinic sub-cells in which the molecular chains are tilted at specific angles determined essentially by the constraints of optimizing chain packing density in the plane perpendicular to the chains. It has however been reported [12,13] that zinc arachidate (ZnA) multilayers do not follow this trend and also exhibit [14] polymorphic phases characterized by different bilayer periods and hence different chain tilt angles. These observations suggest that even in prototypic divalent fatty acid

salt systems, the molecular packing arrangement in the transferred multilayers and its dependence on subphase conditions are not completely understood.

The strong dependence of the layered structure of ZnA multilayers on subphase pH has also led to interest in the investigation of the mixing behaviour of CdA and ZnA, which are systems similar in many respects and yet show very dissimilar organizational behaviour, both at the air–water interface as well as in multilayer structures [15]. The interest is not only from the viewpoint of understanding nano-structured composite organic systems but is also prompted by the possibility of using these mixed multilayer systems as precursors to develop alloy semiconductor nano-clusters such as sulphides, selenides and oxides within organic matrix as well as inorganic alloy nano-crystalline films.

Semiconducting chalcogenide nano-clusters have been formed within the layered matrix through post deposition treatment of precursor LB multilayers with hydrogen sulphide gas [16–22]. The interest in this approach is primarily because the layered structure and molecular order present in the LB multilayers are expected to assist in achieving better control over the size, shape and distribution of nano-clusters. Moreover, the possibility of depositing inorganic–organic nano-composite films with molecular level thickness control opens the possibility of fabricating a wide range of nano-structured devices. LB multilayers of divalent fatty acid salts like cadmium arachidate/stearate have been most extensively used to develop and understand the growth process of semiconducting chalcogenide (e.g., CdS) nano-clusters within the layered matrix of LB films [16]. In comparison, there has been limited work on the growth of ZnS [23–26] and fewer reports [16,27] on Group II mixed sulphides, which have applications in short wavelength opto-electronics, photovoltaics and photo-electrochemical solar cells.

This article reviews the recent work done in our group in the above-mentioned directions.

2. Polymorphic phases in ZnA multilayers

X-ray reflectivity scans from the ZnA multilayers transferred onto quartz substrates at different subphase pH are shown in figure 1. In most cases the multilayers exhibit two types of layered structures corresponding to different bilayer periods, except for the multilayer transferred at pH $\sim$ 6.5. The specular reflectivity scan (figure 1a) for the ZnA multilayers transferred at a nominal subphase pH of 6.5 exhibits a single layered structure with a bilayer period of 4.7 nm (δ-phase). Increasing the subphase pH to 6.8 results in the formation of a two-phase layered structure with bilayer periods of 4.7 (δ-phase) and 5.0 (γ-phase), as seen in figure 1b. On increasing the subphase pH to 7.3, the reflectivity scan (figure 1c) still shows the coexistence of two different layered structures but now with bilayer periods of $\sim$4.7 nm (δ-phase) and $\sim$5.3 nm (β-phase). The ZnA multilayer transferred at a subphase pH of 7.4, however shows drastically different features, as seen in figure 1d. The dominant phase in these multilayers has a period of 5.5 nm (α-phase), together with very weak peaks corresponding to the δ-phase. Multilayers transferred at a higher subphase pH of 7.6 shows the re-emergence of δ-phase together with the γ-phase, as seen in figure 1e.

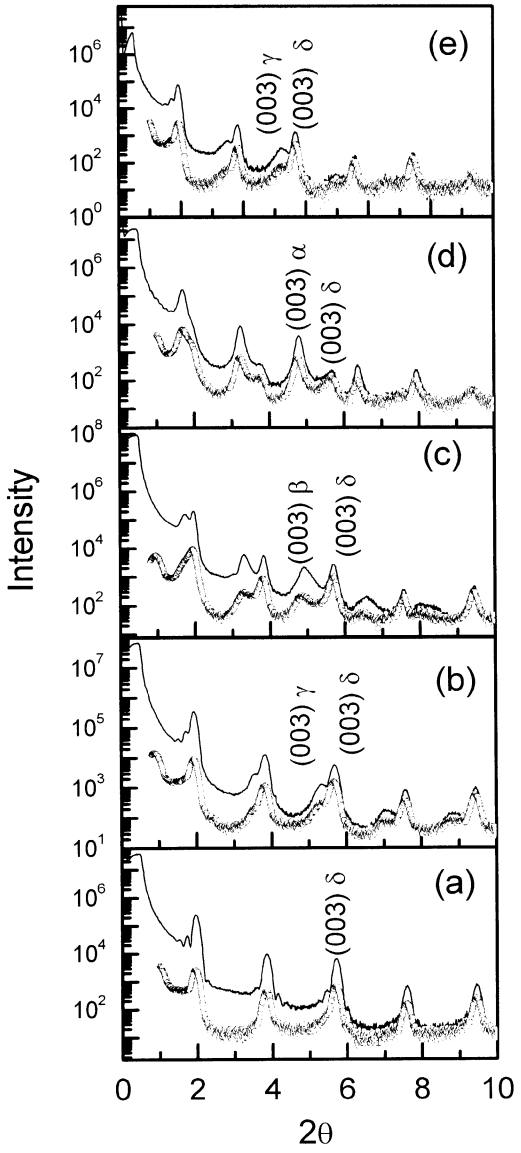

Figure 1. Longitudinal specular (solid line) and off-specular (open circles) scans for the ZnA multilayers transferred at subphase pH values of (**a**) 6.5, (**b**) 6.8, (**c**) 7.3, (**d**) 7.4 and (**e**) 7.6, showing the different types of layered structures present in ZnA multilayers (ref. [30]).

Grazing incidence X-ray diffraction results showing the changes in intralayer molecular packing in ZnA multilayers transferred at different subphase pH values are presented in figure 2. The diffraction pattern of a ZnA multilayer transferred at a subphase pH of 6.5 (figure 2a) consists of a strong peak at 20.05° and a weak, broad peak at 41.55°. The ZnA multilayer transferred at a subphase pH of 6.8 (figure 2b) exhibits broad peaks at 20.05° and 22.95° along with some weak overlapping peaks ∼40°. A similar diffraction pattern was observed for the ZnA multilayer transferred at a subphase pH of 7.2. In contrast, the ZnA multilayer transferred at a subphase pH of 7.3 shows a featureless diffraction scan (figure 2c),

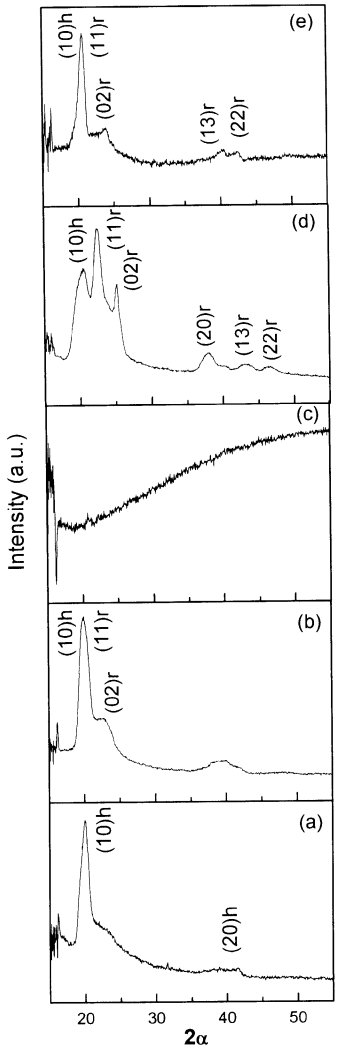

Figure 2. GIXD patterns of ZnA multilayers transferred at subphase pH values of (**a**) 6.5, (**b**) 6.8, (**c**) 7.3, (**d**) 7.4 and (**e**) 7.6, showing the intralayer structure of ZnA multilayers (ref. [30]).

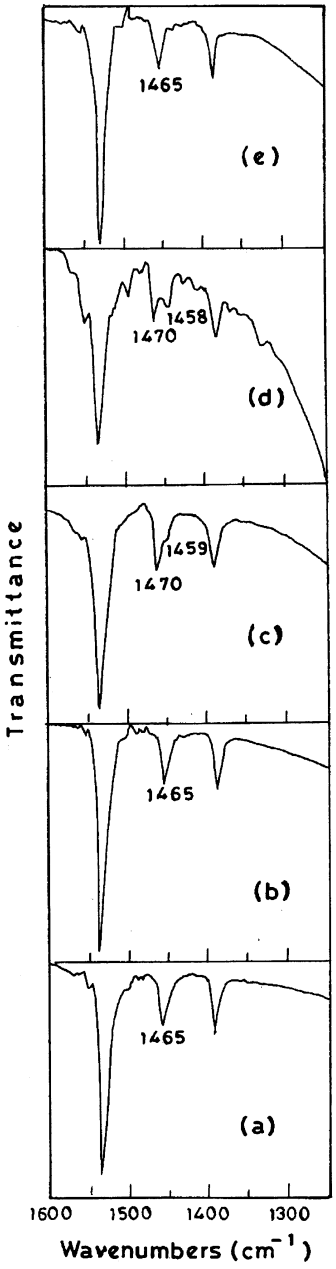

Figure 3. FTIR spectra of ZnA multilayers showing the CH_2 scissoring vibration of ZnA multilayers transferred at subphase pH values of (**a**) 6.5, (**b**) 6.8, (**c**) 7.3, (**d**) 7.4 and (**e**) 7.6, showing the nature of molecular packing in ZnA multilayers (ref. [30]).

indicating a disordered in-plane structure. In sharp contrast, the diffraction pattern from multilayers transferred at a subphase pH of 7.4 (figure 2d), consists of three strong and resolvable peaks at 20.55°, 22.50° and 25.24° along with weak peaks at ∼38°, 43° and 46°. The diffraction pattern from the multilayers transferred at a subphase pH of 7.6 (figure 2e), however, is quite similar to that of the multilayer transferred at a subphase pH of 6.8 (figure 2b).

FTIR spectroscopy can also provide information about the molecular packing in the multilayers, since the CH_2 scissoring mode is known to be sensitive to the intermolecular interactions and has been used to understand molecular packing in long chain compounds [28]. The scissoring vibration band has been monitored for ZnA multilayers transferred on CaF_2 substrates at different subphase pH values and these results are shown in figure 3. Figure 3a and 3b show that for the ZnA multilayers transferred at subphase pH values of 6.5 and 6.8, the CH_2 scissoring vibration exhibits a single band at 1465 cm^{-1}. However, for the multilayer transferred at a subphase pH of 7.3, the CH_2 scissoring vibration (figure 3c) shows a peak at 1470 cm^{-1} with a shoulder at 1459 cm^{-1}. As the subphase pH is increased to 7.4, the CH_2 scissoring vibration clearly splits to form a doublet at ∼1470 and ∼1458 cm^{-1} (figure 3d). However, for a higher subphase pH value of 7.6, the CH_2 scissoring vibration reappears as a singlet ∼1465 cm^{-1} in figure 3e.

The understanding of molecular packing in LB multilayers has generally been on the lines of the work of Kitaigorodskii [11] on solid-state structures of long chain organic compounds. The orthorhombic sub-cell packing proposed by Kitaigorodskii is among the frequently observed packing arrangements in LB multilayers which is also referred to as herringbone packing in which the orientation of the zigzag or long axis of adjacent rows of molecules alternates to facilitate close packing of alkyl chains.

The reflectivity scan shown in figure 1a for the ZnA multilayer transferred at a subphase pH of 6.5 consists of a layered structure characterized by a bilayer period of 4.7 nm, which corresponds to a chain tilt angle of ∼32° (δ-phase). The corresponding GIXD pattern in figure 2a shows a strong low-order peak. The existence of a single low-order GIXD peak as well as the appearance of the CH_2 scissoring band as a singlet indicates that the intralayer molecular packing in the ZnA multilayer is based on a hexagonal layer cell. The GIXD peaks can thus be indexed as (1 0) and (2 0) reflections of a hexagonal lattice with a lattice constant of 0.51 nm, which corresponds to an unusually large mean molecular area of 0.23 nm^2 [13]. This type of molecular packing has not been observed in LB multilayers of divalent fatty acid salts but such loosely packed structures called 'rotator phases' are known to exist in long chain alkanes at higher temperatures [29].

The ZnA multilayer transferred at a subphase pH of 7.4 however shows a drastically different behaviour compared to the above. The reflectivity scan (figure 1d) exhibits the dominance of a layered structure with a bilayer period of ∼5.5 nm (α-phase) along with very weak and broad Bragg peaks corresponding to the δ-phase. The bilayer period of 5.5 nm shows that the arachidate molecules in this case are packed nearly perpendicular to the layer plane. In the corresponding GIXD pattern, out of the three low-order peaks, the peaks at 22.50° and 25.24° correspond to d-values of 0.40 and 0.36 nm, which nearly match with the corresponding values for (1 1) and (2 0) reflections of a rectangular unit cell [13]. The additional peak at

20.55° can again be indexed as the (1 0) reflection of the hexagonal lattice corresponding to a lattice constant of 0.5 nm, and attributed to the δ-phase, which is the weaker component in this case. Based on the above, we attribute the δ-phase to the close packed herringbone structure which consists of arachidate molecules packed in herringbone arrangement in a rectangular layer cell with their chain axis nearly perpendicular to the layer plane. This is the ideal close packed structure described as the R[0,0] sub-cell packing by Kitaigorodskii [11]. The corresponding FTIR spectrum shown in figure 2d strongly supports the GIXR and GIXD results as the scissoring vibration band exhibits a clear doublet, which is characteristic of orthorhombic sub-cell packing with two molecules per unit cell [28]. These results show that in the case of ZnA multilayer transferred at a subphase pH of 7.4, the dominant phase has a close packed molecular packing similar to that usually observed in LB multilayers of divalent fatty acid salts like CdA and PbA [4].

For the ZnA multilayers transferred at all the other subphase pH values the reflectivity scans, the GIXD and FTIR results show the presence of mixed polymorphic phases with characteristic three-dimensional structure, as discussed in detail in ref. [30]. The δ-phase corresponding to the largest alkyl chain tilt angle of $\sim$32°, appears as a single phase around the subphase pH of 6.5 and is found to be stable over the complete pH range (6.5–8.0) investigated. The other phases, namely β, γ and δ appear only in certain ranges of subphase pH.

The dependence of the 3D structure of various phases appearing in ZnA multilayers at different subphase pH reveals an interesting pattern. Towards the lower and higher ends of subphase pH range investigated, the 3D structure tends to acquire a relatively less dense, rotator phase-like molecular packing. Between the two extremes of the subphase pH range investigated, different 3D structures corresponding to close packed arrangements based on orthorhombic subcells, but with alkyl chains tilted from the layer normal, proposed by Kitaigorodskii appear. In a very narrow subphase pH range $\sim$7.4, the ideal close packed herringbone structure dominates. Such a strong dependence of three-dimensional structure on subphase pH has not been observed earlier in divalent fatty acid salt LB multilayers. These studies on ZnA multilayers indicate the limitations of the correlation between metal–ion electronegativity and the molecular packing in multilayers of divalent fatty acid salts. The exhibition of polymorphic phases is possibly due to the complex zinc ion hydrolysis equilibria at different subphase pH existing in the monolayer at air–water interface and its effect on the structure of the transferred multilayers.

3. Mixed CdA–ZnA LB multilayers

This section deals with the effect of CdA molecules on the molecular packing of ZnA, which exhibits a variety of polymorphs with unusual three-dimensional structures, as discussed above.

Figure 4 shows the CH_2 scissoring band for pure and mixed arachidate multilayers. Pure ZnA multilayers (figure 4a) show a broad and nearly symmetric scissoring band, which is dominated by a peak $\sim$1465 cm^{-1}. In contrast, it is noticed from figure 4b that the presence of even 2 mol% CdA in the mixed multilayers diminishes the $\sim$1466 cm^{-1} peak and simultaneously the doublet ($\sim$1470 cm^{-1} and

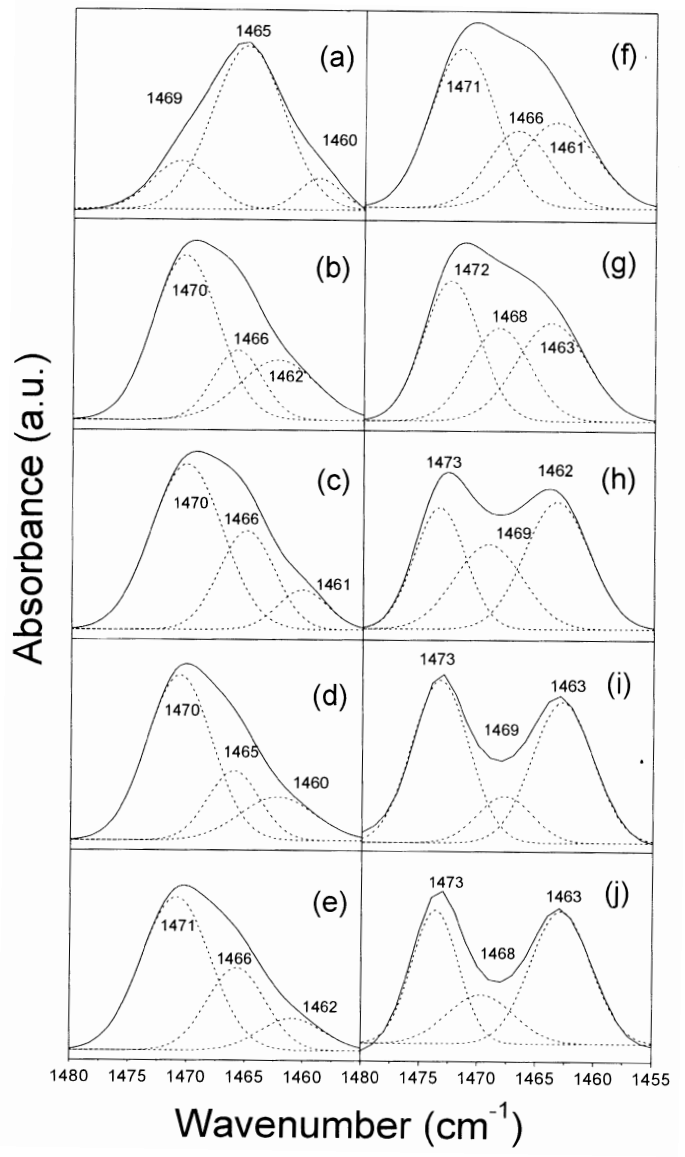

Figure 4. CH_2 scissoring band (s) for (**a**) pure ZnA and mixed multilayers with (**b**) 2 mol% CdA, (**c**) 5 mol% CdA, (**d**) 10 mol% CdA, (**e**) 20 mol% CdA, (**f**) 25 mol% CdA, (**g**) 30 mol% CdA, (**h**) 50 mol% CdA, (**i**) 80 mol% CdA and (**j**) pure CdA (ref. [15]).

$\sim$1462 cm^{-1}) becomes more prominent, with a strong higher frequency component ($\sim$1470 cm^{-1}). Similar features are observed till the case of mixed multilayers with 20 mol% CdA. In the case of mixed multilayers with 20–30 mol% CdA, the lower frequency component of CH_2 scissoring doublet becomes stronger. Subsequently,

for 50 mol% CdA or more (not shown here) the scissoring band doublet dominates and resembles the features associated with pure CdA multilayer.

Figure 5 shows the corresponding X-ray reflectivity scans of these multilayers showing third and higher order Bragg reflections. The average bilayer period for CdA and ZnA were found to be ∼55 Å (α-phase) and ∼47 Å (δ-phase), respectively as discussed above. A shoulder begins to appear in XR pattern of mixed multilayers with 2 mol% of CdA, which clearly develops into a separate set of Bragg peaks for the multilayer with 5 mol% of CdA. This new set of peaks correspond to a layered structure with a bilayer period of ∼51 Å (β-phase). The reduced bilayer period of ∼51 Å indicates that the molecules are tilted by ∼23° from the layer normal. Interestingly, the mixed multilayers with 10–25 mol% of CdA show a single-layered structure (β-phase) with the bilayer period ∼51 Å. Multilayers with 30–50 mol% CdA show the presence of peaks with two different bilayer periods, one corresponding to the α-phase and the other to the β-phase with a bilayer period of ∼52 Å. However, the mixed multilayers with 60 mol% or more CdA showed the presence of a single α-phase similar to pure CdA.

The above results are summarized in figure 6, which shows the approximate phase fields along the composition axis. In this figure, the observed bilayer periods are plotted as a function of the composition of the mixed LB multilayer. The boundaries of phase fields are clearly seen in this phase diagram. The mixed multilayers with 2–5 mol% of CdA show two types of layered structures and molecular packings. The differences in the intensities of the high and low frequencies of the CH_2 scissoring doublet, characteristic of the herringbone packing is attributed to the tilting of molecular chains [31], which is supported by the appearance of a set of Bragg peaks which are attributed to β-phase. However, the presence of a peak at ∼1465 cm^{-1} shows the continued presence of molecular domains with 'rotator'-like 'loose' packing. Interestingly, the mixed multilayers with 10–25 mol% of CdA show a single β-phase in terms of layered structure. However, the FTIR results suggest that the presence of two types of intralayer molecular packings within the same layered structure cannot be completely ruled out. The dominating presence of the layered structure corresponding to a single β-phase is attributed to the influence of CdA molecules on the molecular packing of ZnA-rich mixed multilayers, which results in the reduction of tilt angle to ∼23°, as compared to ∼32° in pure ZnA multilayer. In the concentrations range of 30 to 50 mol% of CdA, multilayers clearly consist of both α- and β-phases. At larger concentrations of CdA, the α-phase corresponding to CdA is dominant. These results have been discussed in detail in ref. [15].

4. Formation of sulphide nano-clusters in LB multilayers

CdA, ZnA and CdA–ZnA mixed LB multilayers have been used as precursors to develop CdS, ZnS and CdS–ZnS alloy nanoclusters, respectively in the confined geometry of LB layered matrix through H_2S exposure at room temperature. Detailed reports on the formation and growth of sulphide nano-clusters and the accompanying changes in the overall structure of the composite multilayers as a function of H_2S exposure have been presented in refs [26,27,32].

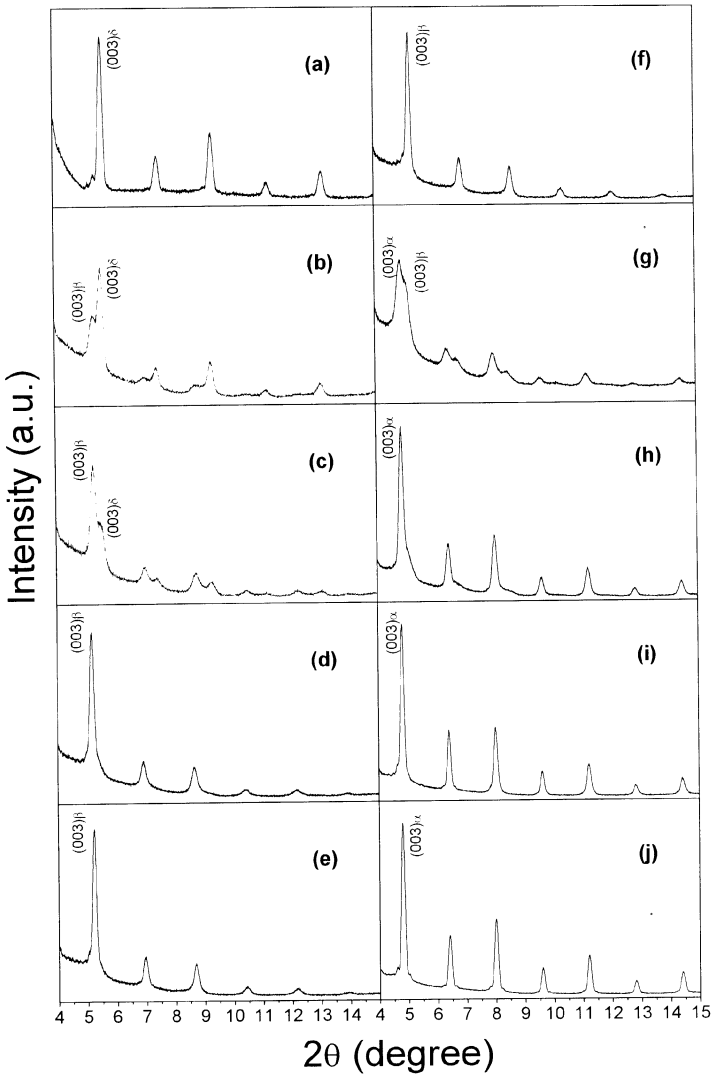

Figure 5. X-ray reflection patterns for (**a**) pure ZnA and mixed multilayers with (**b**) 2 mol% CdA, (**c**) 5 mol% CdA, (**d**) 10 mol% CdA, (**e**) 20 mol% CdA, (**f**) 25 mol% CdA, (**g**) 30 mol% CdA, (**h**) 50 mol% CdA, (**i**) 80 mol% CdA and (**j**) pure CdA (ref. [15]).

Figure 7 shows the UV–Vis absorption spectra of pure CdA and pure ZnA in the as-deposited state and at different stages of H_2S exposures. In both cases, the spectra for 5 min H_2S exposure, exhibit considerable increase in the absorption compared to the as-deposited multilayers. The enhanced absorbance in all these cases indicates sulphide formation in the LB matrix within the first 5 min of H_2S exposure. This behaviour is consistent with FTIR results (not shown here), which

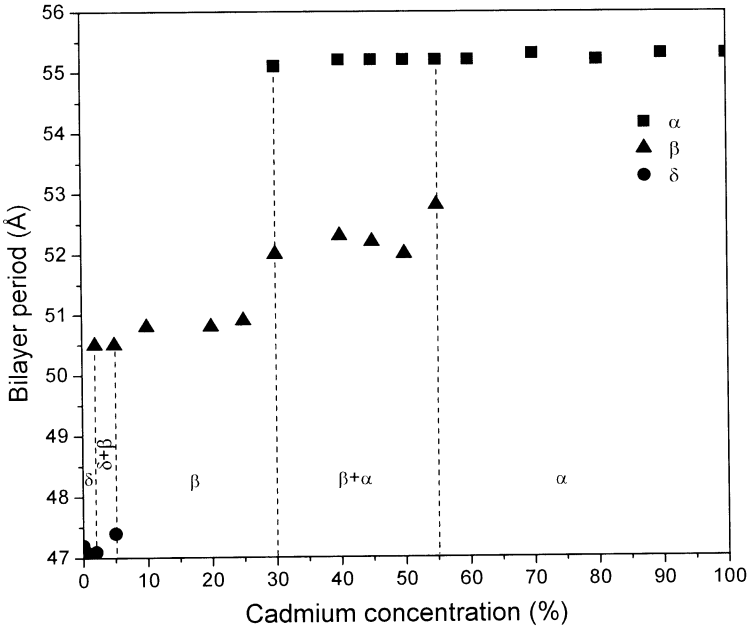

Figure 6. Phase diagram showing a plot of bilayer period with composition, in terms of molar concentration of Cd in subphase (ref. [15]).

also showed that the process of conversion of arachidate salt into arachidic acid is initiated in the early stages of H_2S exposure. In the case of H_2S exposed CdA (figure 4a), the absorption onset is clearly blue-shifted with respect to the bulk absorption edge (515 nm) and a broad hump between 350–400 nm is seen, which is attributed to the excitonic band in CdS [33]. Similarly, in the case of H_2S exposed ZnA (figure 4b), the absorption onset is blue-shifted with respect to the bulk absorption edge (345 nm) and the absorption spectrum exhibits a small and relatively sharp hump at ∼280 nm, which is attributed to the excitonic band of ZnS [34]. The blue shift of the absorption onset and the presence of excitonic peaks in both cases are indicative of quantum confinement effects associated with the formation of CdS and ZnS nanoclusters in the LB matrix in the respective cases. With increase in H_2S exposure duration, up to 3 h, the absorbance continues to increase in all the cases and the absorption onset shows a shift towards longer wavelengths, which may be attributed to the growing size of sulphide nanoparticles with increased H_2S exposure. In all the cases, saturation behaviour is observed in ∼3 h of H_2S exposure, which is consistent with the FTIR and transmission electron microscopy results [26,35].

The UV–Vis spectra of the mixed LB multilayers exposed to H_2S for 5 min and 3 h have been plotted for different compositions in figure 8. It is seen in figure 8b, in which the absorption spectra have been plotted for the saturated condition, that the absorption edge and the excitonic hump continuously and monotonically shifts from pure CdS to pure ZnS spectra indicating the formation of continuous solid solution of $Cd_xZn_{1-x}S$ (in arachidic acid matrix) across the composition

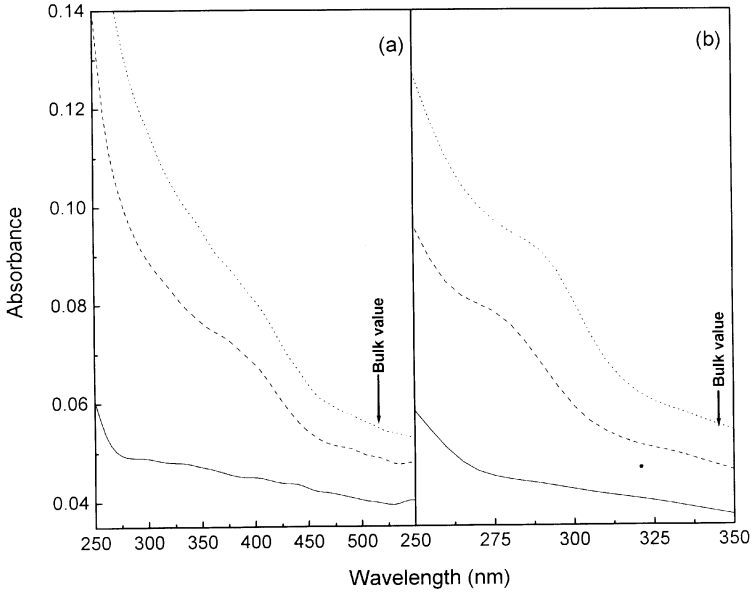

Figure 7. UV–Vis absorption spectra of (**a**) pure CdA multilayer and (**b**) pure ZnA multilayer in the as-deposited state (—) and after H_2S exposed for 5 min (- - -) and 3 h (...). The enhanced absorption indicates the sulphide formation in the arachidic acid matrix. The bulk band gaps for CdS and ZnS are indicated (after ref. [27]).

range. The presence of a hump in the absorption spectra of mixed multilayers is attributed to excitonic absorption and hence, indicates the nanocrystalline nature of the sulphide formed. In comparison, figure 8a shows some unusual features. The spectra for mixed systems cross over that of pure CdS and in most of the region show increased absorption. In particular, the spectra for the $Cd_xZn_{1-x}S$-AA composite film obtained by 5 min H_2S exposure of a 20 mol% ZnA containing precursor multilayer exhibits an excitonic hump at ∼400 nm and absorption onset at ∼450 nm, which is about the same as that for a pure CdS-AA composite film. It is however interesting to note that the excitonic hump in the case of this $Cd_xZn_{1-x}S$-AA nanocomposite film is stronger and sharper than that in the CdS-AA nanocomposite film. These features suggest that compared to the CdS-AA film, in this $Cd_xZn_{1-x}S$-AA film, the nanoclusters formed in 5 min H_2S exposure have a narrower size distribution and are possibly larger in number. Similar features are observed for the $Cd_xZn_{1-x}S$-AA composite films formed from precursor multilayers with 50 and 80 mol% ZnA, though both the absorption spectra are progressively shifted towards the pure ZnS-AA nanocomposite absorption spectra.

The formation of $Cd_xZn_{1-x}S$ alloy nanoclusters in all the mixed multilayers show that CdA and ZnA are present as solid solutions in not only the mixed multilayers with extreme compositions but also in the multilayer with 50 mol% ZnA, which showed the presence of CdA and ZnA type domains, as discussed in §3. Since CdA and ZnA have very different equilibrium packing configurations of molecular

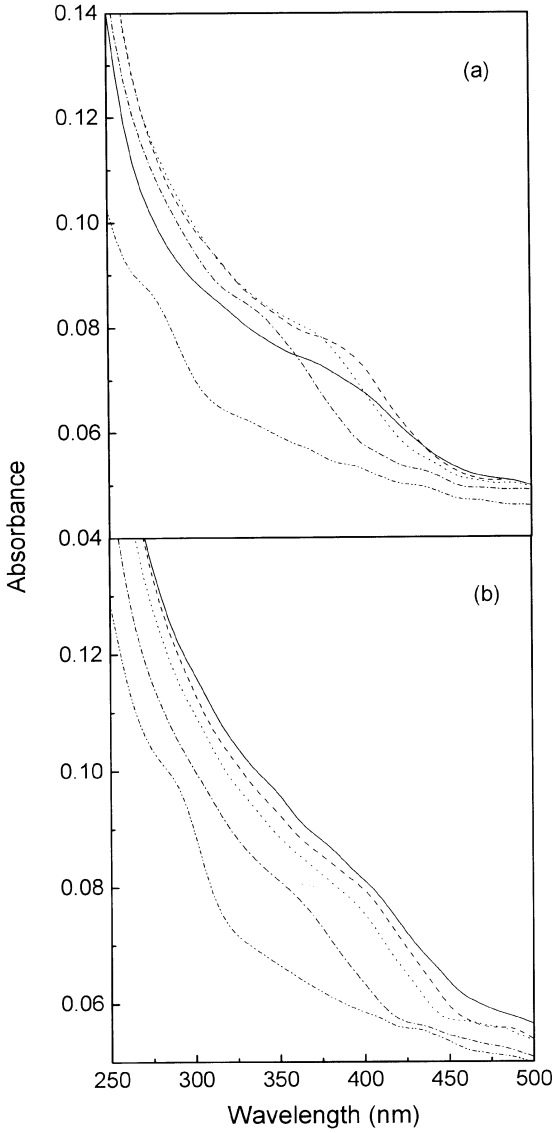

Figure 8. UV–Vis absorption spectra of the multilayers of pure CdA (—), mixed multilayers with 20 mol% ZnA (- - -), 50 mol% ZnA (· · ·), 80 mol% ZnA (-·-·-) and pure ZnA (-··-··-) after (**a**) 5 min and (**b**) 3 h H_2S exposure (ref. [27]).

packing, the mixed multilayers are away from a stable configuration, which possibly facilitates the formation of sulphides more than that in pure CdA or ZnA multilayer systems. The facile formation of alloy sulphide nanoparticles is thus attributed to the metastability of the mixed precursor multilayers.

5. Conclusions

The three-dimensional structure of the ZnA multilayers has an unusually strong dependence on subphase pH, at which the monolayers are transferred. The δ-phase corresponding to the largest alkyl chain tilt angle of $\sim 32^\circ$, appears as a single phase around the subphase pH of 6.5 and is found to be stable over the complete pH range (6.5–8.0) investigated. The other phases, namely β, γ and δ appear only in certain ranges of subphase pH. In a very narrow subphase pH range $\sim$7.4, the ideal close packed herringbone structure dominates, which has not been reported in ZnA multilayers earlier. These results on ZnA multilayers point towards the limited applicability of the correlation between metal–ion electronegativity and the molecular packing in multilayers of divalent fatty acid salts and reveal the complex nature of the relationship between the properties of the monolayer on water surface. Studies on mixed CdA–ZnA multilayers show that the fingerprint of the herringbone type packing starts appearing even at low concentrations of CdA. Interestingly, the mixed multilayers with 10–25 mol% of CdA show a single β-phase in terms of layered structure, which is attributed to the influence of CdA molecules on the molecular packing of ZnA-rich mixed multilayers. The results also show that while a large concentration of ZnA ($\geq$50 mol%) in the mixed multilayers has little effect on the three-dimensional structure of the multilayers, CdA molecules, even at very low concentrations ($<$5%) have a strong influence on the three-dimensional structure of mixed multilayers. H_2S exposure of the pure and mixed arachidate multilayers has been shown to result in the formation of pure and alloy sulphide nanoclusters within the LB layered matrix. The formation and organization of these nanoclusters appear to be strongly influenced by the composition and structure of the precursor arachidate multilayers.

Acknowledgements

This article summarizes the published and ongoing work by our group in the area of organized molecular films. The authors record the contributions by present and past graduate students and post-doctoral fellows as well as collaborators.

References

[1] G Roberts (ed.), *Langmuir-Blodgett films* (Plenum Press, New York, 1990)
[2] A Ulman, *Introduction to ultra-thin organic films* (Academic Press, New York, 1991)
[3] J A Zasadzinski, R Viswanathan, L Madsen, J Garnaes and D K Schwartz, *Science* **263**, 1726 (1994)
[4] D K Schwartz, *Surface Sci. Rep.* **27**, 41 (1997)
[5] J K Basu and M K Sanyal, *Phys. Rep.* **363**, 1 (2002)
[6] R Stömmer, U Englisch, U Pietsch and V Hòly, *Physica* **B221**, 284 (1996)
[7] A Malik, M K Durbin, A G Richter, K G Huang and P Dutta, *Phys. Rev.* **B52**, R11654 (1995)
[8] P Tippmann-Krayer, R M Kenn and H Möhwald, *Thin Solid Films* **210/211**, 577 (1992)

[9] D G Wiesler, L A Feigin, C F Majkrzak, J F Ankner, T S Berzina and V I Troitsky, *Thin Solid Films* **266**, 69 (1995)
[10] J B Peng, G T Barnes and I R Gentle, *Advances in Colloid and Interface Science* **91**, 163 (2001)
[11] A I Kitaigorodskii, *Organic chemical crystallography* (Consultant Bureau, New York, 1961)
[12] R Viswanathan, L Madsen, J A Zasadzinski and D K Schwartz, *Science* **269**, 51 (1995)
[13] N Prasanth Kumar, S Major, S Vitta, S S Talwar, P Dubcek, H Amenitsch, S Bernstorff, V Ganesan, A Gupta and B A Dasannacharya, *Colloids Surfaces* **A198–200**, 75 (2002)
[14] A Dhanabalan, N Prasanth Kumar, S Major and S S Talwar, *Thin Solid Films* **327–329**, 787 (1998)
[15] P K Nayak, S Singh, S S Talwar and R S Srinivasa, *Colloids and Surfaces* **A284–285**, 187 (2006)
[16] J B Peng, G T Barnes, I R Gentle, *Adv. in Colloid and Interface Science* **91**, 163 (2001) and references therein
[17] E S Smotkin, C Lee, A J Bard, A Campion, M A Fox, T E Mallouk, S E Webber and J M White, *Chem. Phys. Lett.* **152**, 265 (1988)
[18] B O Dabbousi, C B Murray, M F Rubner and M G Bawendi, *Chem. Mater.* **6**, 216 (1994)
[19] F Grieser, D N Furlong, D Scoberg, I Ichinose, N Kimizuka and T Kunitake, *J. Chem. Soc. Faraday Trans.* **88**, 2207 (1992)
[20] P Facci, V Erokhin, A Tronin and C Nicolini, *J. Phys. Chem.* **98**, 13323 (1994)
[21] I Moriguchi, I Tanaka, Y Teraoka and S Kagawa, *J. Chem. Soc. Chem. Commun.* 1401 (1991) (Issue No. 19)
[22] A Dhanabalan, H Kudroli, S S Major and S S Talwar, *Solid State Commun.* **99**, 859 (1996)
[23] I Moriguchi, H Nii, K Hanai, H Nagaoka, Y Teraoka and S Kagawa, *Colloids and Surfaces* **A103**, 173 (1995)
[24] F N Dultsev and L L Sveshnikova, *Thin Solid Films* **288**, 103 (1996)
[25] A G Milekhin, L L Sveshnikova, S M Repinsky, A K Gutakovsky, M Friedrich and D R T Zahn, *Thin Solid Films* **422**, 200 (2002)
[26] M Parhizkar, N P Kumar, B Shukla, R S Srinivasa, Satish Vitta, N Kumar, S S Talwar and S S Major, *Colloids Surfaces* **A257–258**, 177 (2005)
[27] M Parhizkar, N Kumar, P K Nayak, S S Talwar, S S Major and R S Srinivasa, *Colloids Surfaces* **A257–258**, 405 (2005)
[28] R G Snyder, *J. Mol. Spectroscopy* **7**, 116 (1961)
[29] E B Sirota and D M Singer, *J. Chem. Phys.* **101**, 10873 (1994)
[30] N Prasanth Kumar, S Major, S Vitta, A Gupta and B A Dasannacharya, *Colloids Surfaces* **A257–258**, 243 (2005)
[31] P A Chollet and J Messier, *Chem. Phys.* **73**, 235 (1982)
[32] N Prasanth Kumar, S N Narang, S Major, S Vitta, S S Talwar, P Dubcek, H Amenitsch and S Bernstorff, *Colloids Surfaces* **A198–200**, 59 (2002)
[33] L E Brus, *J. Chem. Phys.* **80**, 4403 (1984)
[34] R Rossetti, R Hull, J M Gibson and L E Brus, *J. Chem. Phys.* **82**, 552 (1985)
[35] M Parhizkar, *Growth and characterization of semi-conducting sulphide nano-particles and nano-crystalline oxide films obtained from precursor LB multilayers*, Ph.D. Thesis (Indian Institute of Technology Bombay, 2002)